Nano Energy (2014) 6, 59–65

Available online at www.sciencedirect.com

ScienceDirect

journal homepage: www.elsevier.com/locate/nanoenergy

RAPID COMMUNICATION

Harvesting energy from automobile brake in contact and non-contact mode by conjunction of triboelectrication and electrostatic-induction processes

Chang Bao Han[a], Weiming Du[a], Chi Zhang[a], Wei Tang[a], Limin Zhang[a], Zhong Lin Wang[a,b,*]

[a]*Beijing Institute of Nanoenergy and Nanosystems, Chinese Academy of Sciences, Beijing 100083, China*
[b]*School of Material Science and Engineering, Georgia Institute of Technology, Atlanta, GA 30332-0245, USA*

Received 14 February 2014; accepted 18 March 2014
Available online 26 March 2014

KEYWORDS
Triboelectric nanogenerator (TENG);
Energy harvest;
Electrostatic-induction;
Non-contact mode

Abstract
Energy harvesting from moving objects and machines in our daily life, such as automobile and train, is quite important for powering portable electronics, sensor systems and high fuel efficiency. Here, we present a disc-based design that simulates the braking system in an automobile for harvesting energy when the braking pads are both in contact and in non-contact modes. The mechanisms for the design are based on a conjunction use of triboelectrification and electrostatic-induction processes. The static non-mobile charges for driving the free electrons are created by triboelectrification when the two discs of opposite tribo-polarities are in direct contact during the braking action. The process for generating electricity in non-contact mode is due to the electrostatic induction of the existing tribo-charges on the insulating pad. Our approach demonstrates an effective means for harvesting energy from a rotating disc structure during both braking and non-braking processes, with potential application in motor cycles, automobiles, and even moving trains.

Introduction

Energy is urgently needed for the sustainable development of human society in the next few decades and even centuries. Renewable energy has attracted a lot of interest due to its large-scale availability, environmental friendly

*Corresponding author at: Beijing Institute of Nanoenergy and Nanosystems, Chinese Academy of Sciences, Beijing 100083, China.
E-mail address: zlwang@gatech.edu (Z. Lin Wang).

http://dx.doi.org/10.1016/j.nanoen.2014.03.009
2211-2855/

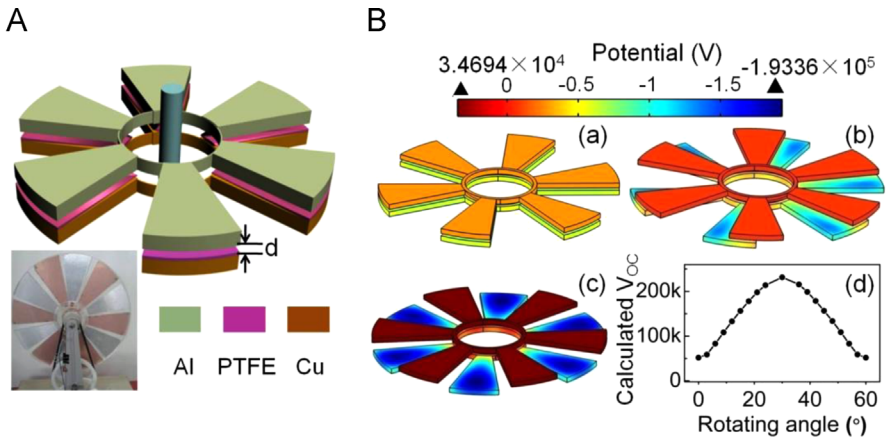

Figure 1 (A) Schematic structure of the disc-based TENG. Inset is a photograph showing the real disc-based TENG. (B) Finite-element simulation of the potential distribution for the discs (d=5 mm) at different relative rotation angles: (a) 0°, (b) 12°, (c) 24°. (d) is the simulated maximum potential difference between PTFE and Al layer as a function of relative rotation angle.

nature and sustainability [1-4]. The most popular green energy is solar energy, wind energy and hydraulic power [5-7]. Take hydraulic energy as an example; it is mainly converted into electricity via the electromagnetic induction process [8] as first discovered by Faraday. This has been the most important approach for mechanical energy conversion. Although piezoelectric effect [9,10] and electrostatic effect [11] have been used for converting mechanical energy into electricity at small scale, their efficiencies are rather low.

Recently, a new and innovative approach based on the triboelectrification effect has been invented for converting small-scale mechanical energy into electricity [12,13]. A triboelectric nanogenerator (TENG) has been demonstrated for harvesting energy in the following modes: contact-separation [14,15], lateral sliding [16,17], and double-electrode or single electrode [18]. Disc-based TENG has been demonstrated based on contact electrification [16], which raises about the wearing of the contact materials with the increase in working load and time. A common characteristic of these modes requires a direct contact of the two materials in order to harvest energy, which may give rise to issues such as durability, life time and stability for the TENG. For example, the continuous friction in the lateral sliding mode disk TENG will produce a large amount of heat and accelerate material depletion, thereby restricting its wide applications. Now let us consider a practical situation such as a disc-based braking system in an automobile. During braking, the brake pads are forced to be in contact with the rotating disc, but in the non-braking situation, for most of the time, the pad may be a bit away from the disc. Although the demonstrated TENG can harvest energy from a disc brake system during tight contact, an approach is missing for the case when the pad is off the disc with minimized friction.

Here, we demonstrate a disc shape TENG that can harvest energy in a brake system during both contact and non-contact modes. In contact mode, the TENG operates in the lateral sliding mode that is dominated by a parallel triboelectrification and electrostatic-induction processes. In non-contact mode, the TENG relies on electrostatic induction for energy harvesting. The conjunction operation of the TENG in the two modes opens a new approach for harvesting energy from a disc-based brake system, with potential applications in motor cycles, automobiles, and even moving trains.

Experimental section

The basic design of the TENG is shown in Figure 1(A). Six fan-shaped Al foils were connected by an annular electrode as an electrode/induction layer. A polytetrafluoroethylene (PTFE, 100 μm-thick) was fabricated to have the same shape as the Al layer. On the backside of the PTFE layer, a 300 nm - thick copper layer was deposited that serves as another electrode. The Al layer was attached to a polymethyl methacrylate (PMMA, 5 mm-thick) disc substrate on one side of the TENG; and the PTFE-Cu layers were attached to another PMMA disc substrate. Both parts can freely rotate with respect to each other in both contact and non-contact modes to simulate the braking and non-braking modes of a brake pad, respectively. The spacing between the Al layer and the PTFE film is defined as d. The switch between electrostatic-induction and triboelectrication can be achieved by adjusting the spacing d. All of the fan-shaped structures have an external diameter of 230 mm, inner diameter of 71 mm and a radial angle of 24°.

Result and discussion

Working mechanism of the TENG

The electric potential distribution in the Al layer and the PTFE layer at different relative rotation angles were first simulated using COMSOL. The triboelectric charge density on the surfaces of Al and PTFE was first set as $\pm 90\ \mu C/m^2$, respectively, and the spacing (d) between the two was set as 5 mm. Figure 1(B) shows the potential distribution on discs at three typical relative rotation angles: 0°, 12° and 24°. The maximum potential drop between the Al and PTFE

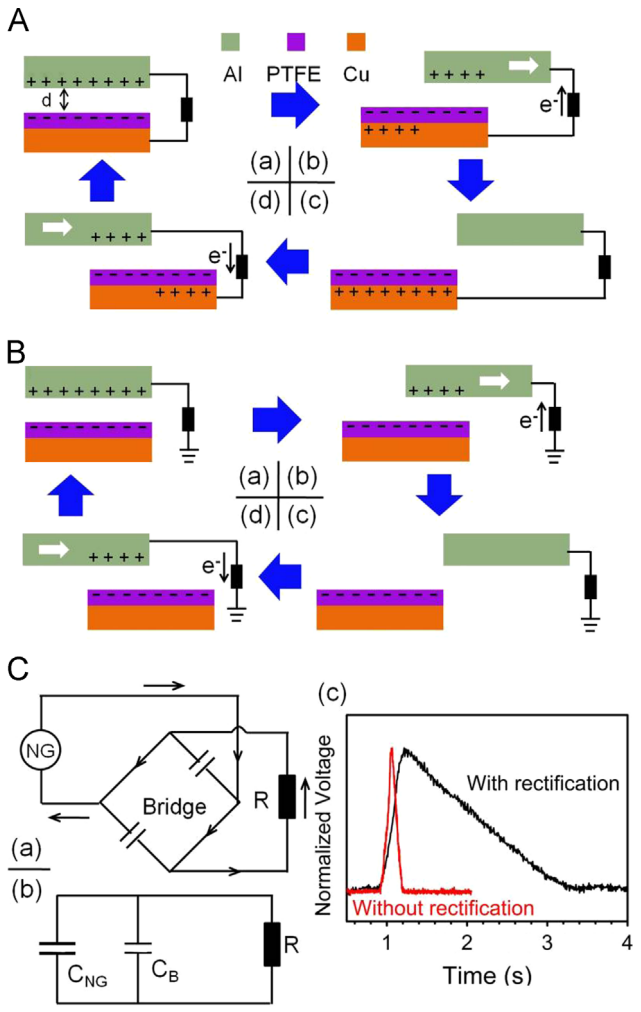

Figure 2 (A) and (B) are the sketches for the electricity generation process in a full cycle for double-electrode and single-electrode TENG at the non-contact mode. (C) An equivalent circuit testing process and results: (a) the rectifier bridge at reversely biased state acting as a capacitor; (b) the TENG and rectifier bridge working as the capacitors of C_{NG} and C_B, respectively; (c) normalized output voltage with and without rectification for a non-contact mode TENG.

layers was calculated and is plotted in Figure 1(B-d). The highest potential difference occurs when the two layers are completely mismatched [16].

The working mechanism of the TENG is illustrated in Figure 2(A) for the double-electrode case. At the initial position, we assumed that the PTFE and Al had been in contact so that the two surfaces were charged negative and positive, respectively, due to the triboelectrification process. Then, the two surfaces are separated for a distance *d* and the Al film is right above the PTFE layer (Figure 2(A-a)). When the PTFE layer slides in parallel to the Al layer for a small angle (Figure 2(A-b)), the free electrons in the Cu electrode beneath the PTFE will flow to the Al layer to balance/screen the non-mobile triboelectric charges in the PTFE layer. This process continues until the two films are completely mismatched (Figure 2(A-c)). When the Al layer continues to rotate and starts to overlap with the next PTFE layer on the other segment of the disc (Figure 2(A-d)), the free electrons in the Al layer will flow back to the corresponding Cu electrode beneath the PTFE layer. This is a cycle of electricity generation.

Alternatively, if the Al electrode is connected to the ground, it is a single-electrode TENG (Figure 2(B)), and the electricity generation process can be explained by the same token. The only difference is that the electrons flow between the Al layer and the ground.

This output is an alternating current (AC) signal, and it can be converted into direct current (DC) signal using a rectification bridge. When the rotation frequency is high, the rectified current appears like a constant DC, for the following reason. Using an equivalent circuit model, a diode may be taken as a capacitor at a reversely biased case [19]. As shown in Figure 2(C-a), if the electrons flow through the bridge, two diodes are forward biased but the other two are reversely biased. So the two reversely biased diodes are represented by capacitor C_B. Also, the TENG can be regarded as a capacitor C_{NG}. If $C_{NG} \gg C_B$, the capacitance is dominated by C_{NG}. If C_{NG} is comparable to C_B, the filtering effect of the rectification bridge becomes noticeable for discharging C_B [20]. In our current work, the measured capacitance of C_{NG} is about 100 pF and the C_B is 50 pF. Figure 2(C-c) is the normalized open-circuit voltage (V_{OC}) curves for a cycle (Figure 2(A)(c)→(d)→(a)→(b)→(c)). The discharge time constant of the V_{OC} with the rectifier bridge is about 2.1 s, which is much longer than the 0.15 s without rectification. The results reveal that our device with a rectifier bridge would achieve an approximate constant DC output when the rotation frequency gets higher.

Effect of electrode design on performance

To compare the output performance for non-contact TENG at different electrode modes, a double-electrode (Al-Cu) and two single-electrode (Al-Ground and Cu-Ground) TENGs were tested at a rotating speed (*R*) of 900 r/min when the space between Al and PTFE is set at 4 mm. A rectifier bridge (type: KBP210) was introduced during the testing process. As shown from Figure 3(A), the output V_{OC} and short-circuit current (J_{SC}) are a DC signal rather than an AC signal. It means that the capacitance of the rectifier bridge is well matched with the TENG. At the double-electrode mode, the V_{OC} is kept at about 60 V and the J_{SC} density reaches 0.86 mA/m^2. When the other electrode of Cu or Al was connected to the ground (single-electrode mode), the V_{OC} reduces partially but the J_{SC} drops by more than half. This is because the potential difference between Al and Cu at the double-electrode mode is higher than that between Al-Ground (or Cu-Ground) and the ground in the single-electrode mode. When introducing different loading resistances, the output voltage and current were measured and they are shown in Figure 3(B). With the increase in loading resistance, the output voltage increases and the output current density decreases [16,18,21]. Therefore, the effective output power for the non-contact TENG has an optimal value and the measured date as well as fitted curves are shown in Figure 3(B-d). The maximum output power density reaches 5.7 mW/m^2 at a loading of 20 M Ω for the

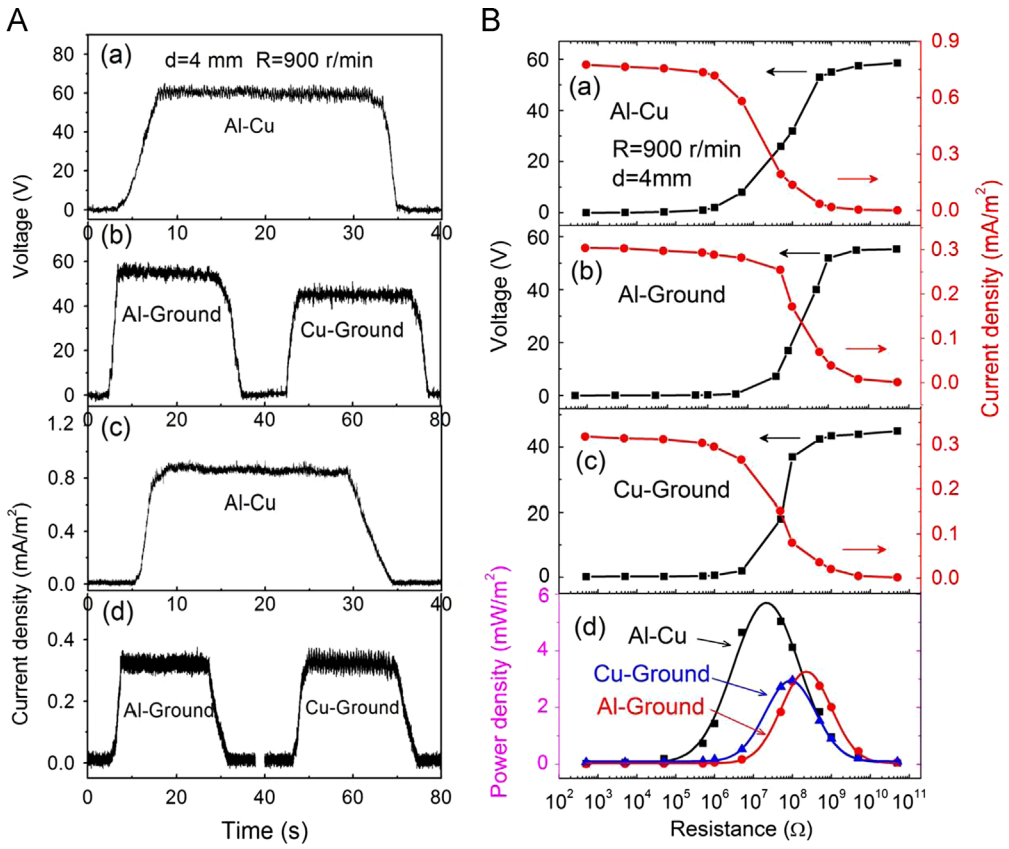

Figure 3 Performance comparison of non-contact TENG for the double-electrode (Al-Cu) and single-electrode mode (Al-Ground and Cu-Ground) at gap space d=4 mm and rotating speed R=900 r/min. (A) The measured V_{OC} and J_{SC} change versus times at different modes: (a)(c) double-electrode (Al-Cu), (b)(d) single-electrode (Al-Ground, Cu-Ground). (B) The corresponding output voltage, current density and power density at different external load resistances for different modes of operations.

double-electrode mode, while the maximum for single-electrode mode is achieved at 100 M Ω.

Effects of rotating speed and gap distance on performance

When a relative rotation occurs between Al and PTFE around the central axis, the V_{OC} and J_{SC} will produce a periodic variation according to our analysis in section "Working mechanism of the TENG". Because the rectifier bridge in the circuit worked as a capacitor C_B (Figure 2(C-b)), the time of charge transfer at a cycle (0→60°) will be extended notably when C_B is comparable to C_{NG}. The single cycle test shows that the time (t_0) of V_{OC} or J_{SC} dropping from the maximum to 95% is more than 0.12 s (Figure 2(C-c)), corresponding to a frequency f_0 of 83 r/min (f_0=60/(6t_0)). Therefore, when the rotation speed is larger than f_0, the output signal would present an approximately constant DC feature. Thus, the performance of the non-contact TENG in the double-electrode mode was tested with the R varying from 90 to 1200 r/min when d=5 mm (Figure 4(A) and (B)). Apparently, the DC features for V_{OC} and J_{SC} were realized at different speeds. With the increase of rotation speed R, the V_{OC} is almost a constant and kept at about 45 V, but the J_{SC} increases linearly, which is a result of reduced elapse time for each cycle while the total transported charges remain constant [16].

In order to study the effect of spacing between the two discs (Al and PTFE) on the TENG output, different d with an identical R (900 r/min) were carried out. As shown from Figure 4(C) and (D), an increase in the gap distance d from 1 mm to 5 mm leads to a simultaneous reduction of both voltage and current, but the decay slope is not too large. The trend is obviously originated from the inverse proportional relationship between the induced charge density on Al and d according to the electrostatic principle. When the d reduces to 0, it is the contact mode TENG and the V_{OC} or J_{SC} all reach the maxima (the inset of Figure 4(C-b)). Here, the V_{OC} and J_{SC} are still the superposition of single peaks because the C_{NG} is as high as 10 μF, which is far more than C_B and agrees to the lateral sliding mode disk TENG [16]. In this situation, the rectifier bridge did not function as a discharging or filtering capacitor but as a switch. The insets in Figure 4(B) and (C) are the snapshots of the LEDs that are being lit up by the electricity generated at the corresponding rotation speed and gap spacing, the brightness of which indicates the magnitude of the output power.

According to the load testing in section "Effects of rotating speed and gap distance on performance", the matched load resistance at double-electrode mode for the maximal output power is 20 M Ω. So the TENG was tested at d=1 mm and R=900 r/min with a load of 20 M Ω (Figure S1).

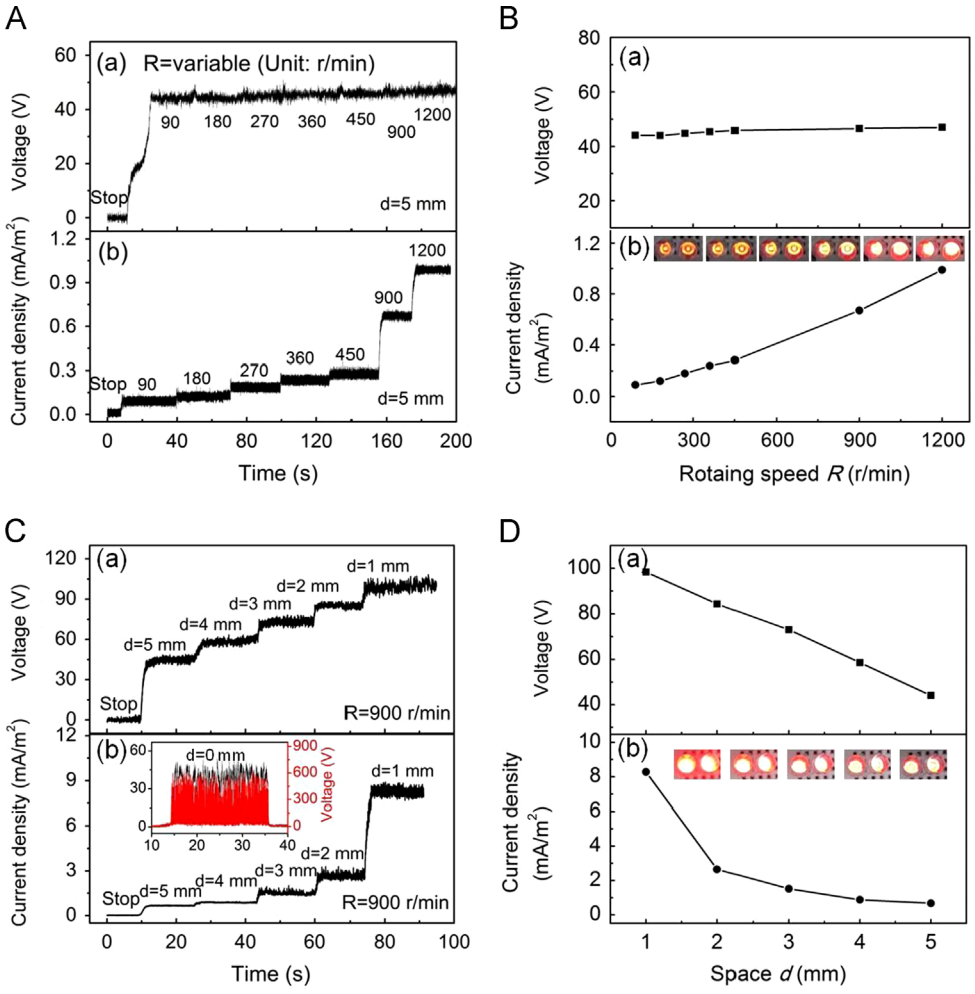

Figure 4 (A) The measured V_{OC} (a) and J_{SC} (b) change versus times at different rotating speeds (d=5 mm). (B) The plot of V_{OC} (a) and J_{SC} (b) versus rotating speed at d=5 mm. (C) The measured V_{OC} (a) and J_{SC} (b) change versus times at different spaces with R=900 r/min. (D) The plot of V_{OC} (a) and J_{SC} (b) versus space (R=900 r/min). The inset in Figure 4 (C)(b) is the measured V_{OC} (a) and J_{SC} (b) change versus times at d=0 mm with R=900 r/min (lateral sliding mode TENG). The insets in (B) and (C) are the snapshot images of LEDs at the corresponding speed and gap spacing.

The results show that an excellent output voltage of 65 V, current density of 3.4 mA/m^2 and power density of 221 mW/m^2 were achieved at non-contact mode.

TENG operated in coupled mode

The non-contact TENG can harvest energy at minimized material wearing if it is applied for practical applications, which is important for the durability, life time and stability of the TENG as a sustainable power source. Here, we simulate the operation of an automobile brake using the contact and non-contact modes of TENG. A simulative brake pad TENG was fabricated and the electric generation mechanism during the braking process is illustrated in Figure 5(A). Firstly, the two pads are separated ($d \neq 0$) and it is a TENG in non-contact mode. When the two rotating discs approach each other, the induced charges will flow from Cu to Al for generating an electric current to fully screen the tribo-charges on PTFE (①) (Figure 5(A) (a)→(b)). Then the two discs are in full contact (d=0), and the relative sliding between the two will generate the current pulses of opposite polarity (② and ③) [17]. When the force for braking is released, the two discs begin to separate and another induced current peak is produced (④). The inset in Figure 5(A) is the measured J_{SC} curves for a full period of braking in accordance with the proposed mechanism. In this process, the current density generated from non-contact TENG is observably lower than that from the contact mode TENG because of the difference in transferring triboelectric charges and the dependence of electrostatic induction on gap distance. It is important to note that the triboelectric charges remain on the insulator surface for hours without much leakage, so that their subsequent induction is possible.

Figure 5(B) presents the measured J_{SC} after rectification for multiple cycles of braking (contact mode) and non-braking (non-contacting mode): from stop status to rotating and then to periodic braking. When the discs rotate at a speed of 900 r/min with d=3 mm, the induced J_{SC} reaches 1.5 mA/m^2, but a significantly enhanced J_{SC}, up to 43 mA/m^2, was achieved after braking. The corresponding peak V_{OC} is

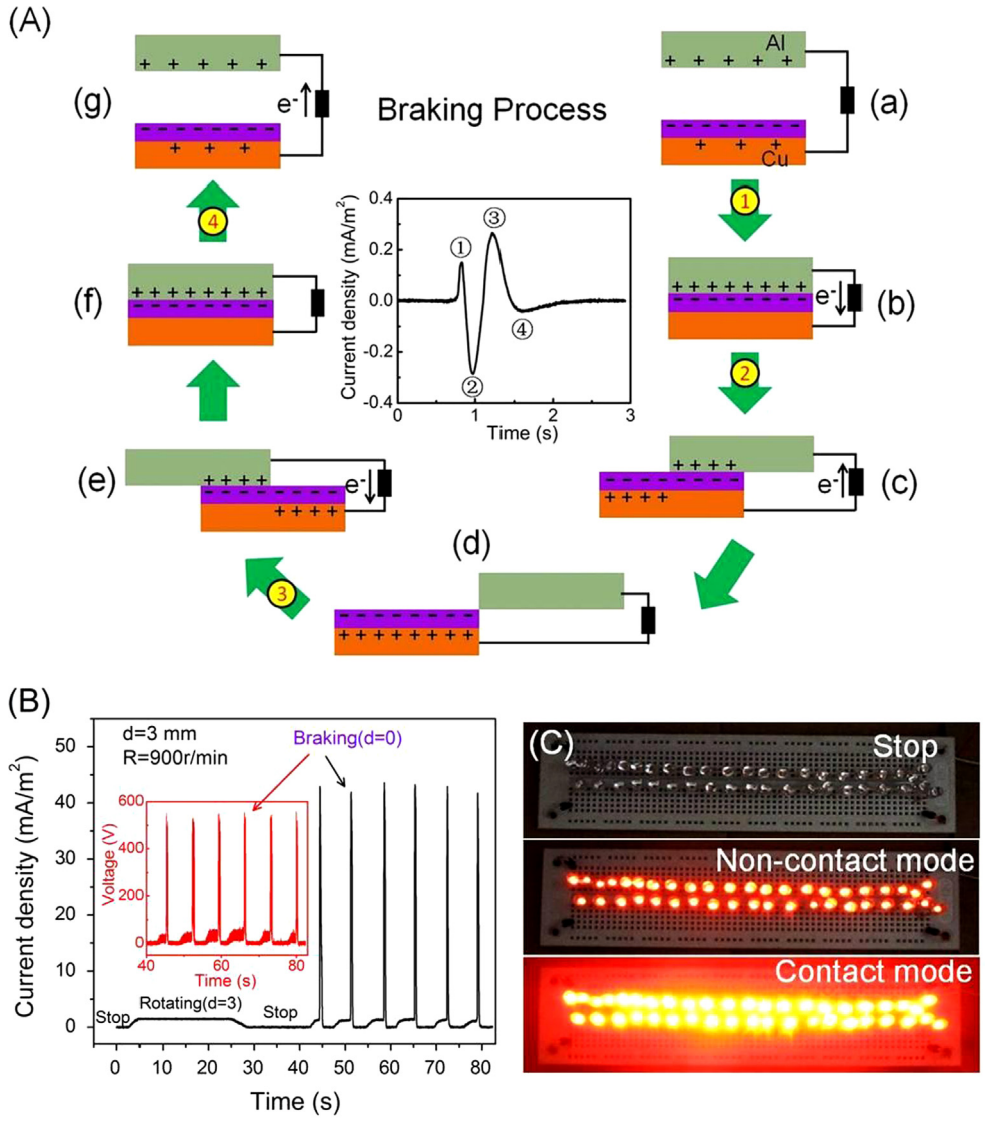

Figure 5 Simulating the electricity generation in a braking process using a TENG. (A) The basic mechanism of electricity generation process in a braking cycle. The inset is the measured J_{SC} change versus times, and the four current peaks corresponding to four electricity generation processes in (A). (B) The measured J_{SC} curve at different situations: stop, rotating and braking (d=3 mm and R=900 r/min). The inset is the corresponding V_{OC} curve. (C) Photographs of a continuous luminescence process for red LEDs when rotating (non-contact mode) and a flashlight when braking (contact mode).

also greater than 500 V when braking (shown in the inset of Figure 5(B)). The output signals can also be confirmed by the brightness of the red LEDs (Figure 5(C)).

Conclusion

We present a disc-based design that simulates the braking system in an automobile for harvesting energy when the braking pads are in both contact and non-contact modes. The design is based on a sequential triboelectrification process and electrostatic induction process so that electricity can be generated when the two discs are in both contact and non-contact modes. In the contact mode, the output voltage is ~540 V and the output current density is 43 mA/m^2 (open circuit situation). In the non-contact mode, the output voltage reaches 65 V and the output current density is 3.4 mA/m^2 and a power density of 221 mW/m^2 was arrived at the matched load resistance of 20 M Ω. Although there is a major difference in the output magnitude in both modes, one must realize that there is a much reduced friction in the non-contact mode, so that the true energy conversion efficiency is truly high in the non-contact mode. Our demonstrated approach provides a realistic technology for harvesting energy from rotating machines, such as bicycles, automobiles, and trains.

Acknowledgments

Thanks for the support from the “Thousands Talents” Program for pioneer researcher and his innovation team, China. Thanks to Fei Xue, Mengxiao Chen and Chao Yuan for their assistance in the preparation of the device.

Appendix A. Supporting information

Supplementary data associated with this article can be found in the online version at http://dx.doi.org/10.1016/j.nanoen.2014.03.009.

References

[1] J.A. Turner, Science 285 (1999) 687–689.
[2] I. Dincer, Renew. Sustain. Energy Rev. 4 (2000) 157–175.
[3] H. Lund, Energy 32 (2007) 912–919.
[4] M. Hitzeroth, A. Megerle, Renew. Sustain. Energy Rev. 27 (2013) 576–584.
[5] S.A. Sherif, F. Barbir, T.N. Veziroglu, Sol. Energy 78 (2005) 647–660.
[6] A. Khaligh, O.C. Onar, Energy Harvesting: Solar, Wind, and Ocean Energy Conversion Systems, CRC Press, Boca Raton, 2010.
[7] P. Nema, R.K. Nema, S. Rangnekar, Renew. Sustain. Energy Rev. 13 (2009) 2096–2103.
[8] A. Herzenberg, F.J. Lowes, Philos. Trans. R. Soc. London Ser. A-Math. Phys. Sci. 249 (1957) 507–584.
[9] Z.L. Wang, J.H. Song, Science 312 (2006) 242–246.
[10] C. Chang, V.H. Tran, J. Wang, Y.-K. Fuh, L. Lin, Nano Lett. 10 (2010) 726–731.
[11] R.G. Herb, D.B. Parkinson, D.W. Kerst, Phys. Rev. 51 (1937) 75–83.
[12] Z.L. Wang, ACS Nano 7 (11) (2013) 9533–9557.
[13] F.R. Fan, Z.Q. Tian, Z.L. Wang, Nano Energy 1 (2012) 328–334.
[14] X.-S. Zhang, M.-D. Han, R.-X. Wang, F.-Y. Zhu, Z.-H. Li, W. Wang, H.-X. Zhang, Nano Lett. 13 (2013) 1168–1172.
[15] G. Zhu, Z.-H. Lin, Q. Jing, P. Bai, C. Pan, Y. Yang, Y. Zhou, Z.L. Wang, Nano Lett. 13 (2013) 847–853.
[16] L. Lin, S. Wang, Y. Xie, Q. Jing, S. Niu, Y. Hu, Z.L. Wang, Nano Lett. 13 (2013) 2916–2923.
[17] G. Zhu, J. Chen, Y. Liu, P. Bai, Y.S. Zhou, Q. Jing, C. Pan, Z.L. Wang, Nano Lett. 13 (2013) 2282–2289.
[18] Y. Yang, H. Zhang, J. Chen, Q. Jing, Y.S. Zhou, X. Wen, Z.L. Wang, Acs Nano 7 (2013) 7342–7351.
[19] J. Rodríguez, P. Lezana, S. Kouro, A. Weinstein, 11 – single-phase controlled rectifiers, Power Electronics Handbook, Third Edition, Butterworth-Heinemann, Boston, 2011.
[20] Y.-S. Lee, M.H.L. Chow, 10 – diode rectifiers, Power Electronics Handbook, Third Edition, Butterworth-Heinemann, Boston, 2011.
[21] S. Wang, L. Lin, Y. Xie, Q. Jing, S. Niu, Z.L. Wang, Nano Lett. 13 (2013) 2226–2233.

Dr. Changbao Han received his Ph.D. degree from Zhengzhou University in 2012. He first fabricated the GaN/Si nano-heterostructure array LEDs and realized its near-infrared light emission with high monochromaticity by band-gap engineering. His research interests include the synthesis of semiconductor nanomaterials, photoelectric device and applications of triboelectric nanogenerator.

Weiming Du is a second-year postgraduate. She received her bachelor's degree in 2007. After graduation, she worded in the 13th research Institute of China electronics technology group corporation as a technologist. Her research interests are nanogenerator, flexible electronics, and their applications in driving electronics, active sensor and flexible sensor.

Dr. Chi Zhang received his Ph.D. degree from Tsinghua University in 2009. After graduation, he worked in Tsinghua University as a postdoc research fellow and NSK Ltd., Japan as a visiting scholar. His research interests are nanogenerator as active micro/nano-sensors, self-powered MEMS/NEMS, flexible electronics, and their applications in sensor networks and human-machine interaction.

Dr. Wei Tang received his Ph.D. degree from Peking University in 2013. He visited CMI of EPFL to participate in a Swiss-China joint Project in 2012. His research interests are micro/nano-devices, principle investigation of triboelectric nanogenerators, structure optimization, power transformation & management, and self-powered wireless sensing network.

Limin Zhang received her undergraduate degree from Hebei University of Technology in 2012, and now she is a second-year graduate student. Her research interests are piezoelectric nanogenerator and triboelectric nanogenerator, especially focusing on nanogenerators as active micro/nano-sensors, flexible electronics and their applications in sensor networks and human-machine interaction.

Zhong Lin (ZL) Wang received his Ph.D. from Arizona State University in physics. He now is the Hightower Chair in Materials Science and Engineering, Regents' Professor, Engineering Distinguished Professor and Director, Center for Nanostructure Characterization, at Georgia Tech. Dr. Wang has made original and innovative contributions to the synthesis, discovery, characterization and understanding of fundamental physical properties of oxide nanobelts and nanowires, as well as applications of nanowires in energy sciences, electronics, optoelectronics and biological science. His discovery and breakthroughs in developing nanogenerators established the principle and technological roadmap for harvesting mechanical energy from the environment and biological systems for powering a personal electronics. His research on self-powered nanosystems has inspired the worldwide effort in academia and industry for studying energy for micro-nano-systems, which is now a distinct disciplinary in energy research and future sensor networks. He coined and pioneered the field of piezotronics and piezo-phototronics by introducing piezoelectric potential gated charge transport process in fabricating new electronic and optoelectronic devices. Details can be found at: www.nanoscience.gatech.edu.